ELSEVIER

Journal of Chromatography B, 782 (2002) 127–135

JOURNAL OF CHROMATOGRAPHY B

www.elsevier.com/locate/chromb

Review

Single-molecule reader for proteomics and genomics

Jan Hesse[a], Christian Wechselberger[b], Max Sonnleitner[b], Hansgeorg Schindler[a], Gerhard J. Schütz[a,*]

[a]*Biophysics Institute, Johannes-Kepler-University Linz, Altenbergerstrasse 69, A-4040 Linz, Austria*
[b]*Center for Biomedical Nanotechnology, Upper Austrian Research GmbH, Scharitzerstrasse 6-8, A-4020 Linz, Austria*

Abstract

Recent developments in ultrasensitive fluorescence microscopy enabled the detection and detailed characterization of individual biomolecules in their native environment. New types of information can be obtained from studying individual molecules, which is not accessible from ensemble measurements. Moreover, this methodological advance matches the need of bioscience to downscale the sample amount required for screening devices. It is envisioned that concentrations as low as ~1000 molecules contained in a sample of 1 nl can be detected in a chip-based assay. In this review, we overview state-of-the-art single molecule microscopy with respect to its applicability to ultrasensitive screening. Quantitative estimations will be given, based on a novel apparatus designed for large area screening at single molecule sensitivity.

Keywords: Reviews; Proteomics; Genomics; Single-molecule reader

Contents

1. Introduction

Insights into biological properties of cells are commonly gained through the determination of RNA and protein expression profiles. Phenotypic aberrations have been shown to be directly linked to the expression of specific genes or proteins [1]. These correlations represent the basis for current assays in bioscience and medical diagnostics. Unambiguous identification of aberrant phenotypes, still, remains a

*Corresponding author. Tel.: +43-732-2468-9265; fax: +43-732-2468-9280.
E-mail address: gerhard.schuetz@jku.at (G.J. Schütz).

1570-0232/02/$ – see front matter
PII: S1570-0232(02)00552-4

difficult task. Large amounts of sample material are required in order to yield detectable signals. This requirement is not limiting for the study of model systems, which use cell culture systems. In contrast, only minute amounts of tissue or body fluids are available for routine sample screening in medical diagnostics. For nucleic acid detection, the problem of limited sample size can be bypassed using PCR-based amplification. Such methods, however, often lead to complications due to cross-contamination of sample material, and distorted statistical outputs. On the contrary, for the analysis of proteins only indirect amplification methods exist [2].

From this line of argumentation, an ultra-sensitive detection device is mandatory for any future genomics and proteomics platform. Steps towards this direction have been taken using gel electrophoresis [3], which allowed to quantify protein expression on single cells. In a different approach, highly sensitive protein-chip read-out has been accomplished using excitation via a planar wave-guide [4]. Recent advances in fluorescence detection techniques extended the range of sensitivity down to the level of single dye molecules. Using such devices, reliable quantification of the number of analytes immobilized on a chip surface is possible at a high dynamic range, from $\sim 10^6$ molecules down to 1 molecule per 100 μm^2. In order to make such detection devices applicable for diagnostic purposes, high throughput capability has to be ensured. Scanning speeds up to 1 cm^2 within ~15 min are feasible with current detectors. In this review, we summarize recent developments in ultra-sensitive high-throughput fluorescence detection in view of its applicability to current demands in genomics and proteomics.

2. Methods for the detection of single molecules

Pioneering work for the detection and characterization of single fluorescent molecules was performed in the early 1990s by several groups, which studied the spectroscopic behavior of single chromophores embedded in condensed matter at low temperature [5,6]. These studies pushed the limits of sensitivity, however, the systems investigated were far from being biologically relevant. Milestones on the way to applicability in bioscience were reached during the last decade, including single molecule detection at room temperature [7], in buffer [8–10], and in living cells [11–13].

Currently, two strategies are followed for establishing high-throughput screening devices at single molecule sensitivity: firstly, fluorescent molecules in solution are detected by a stationary excitation and detection system. Most prominently, confocal devices have been applied to restrict the detection volume down to a few femtoliters [14]. Using avalanche photodiodes as detectors allows to study the fluorescence intensity, fluorophore transition rates and spatial mobility. Combination of multiple detectors gains additional information about spectral properties. Such devices have been extensively used to study binding kinetics [15], conformational fluctuations [16], spectroscopic transitions [17,18] and molecular mobilities [19] using fluorescence correlation spectroscopy (FCS, for a review see Ref. [20]). This information can be assessed within a few seconds, rendering FCS a promising tool for miniaturized high-throughput screening [21]. Fluorescent molecules in solution have been directly imaged on a camera, as they were passing through the defocused excitation beam. The largely increased observation area, compared to a point detector as used for FCS, highly increases detection speed, which has been utilized for DNA fragment sizing [22]. Constant flow of the solution and hydrodynamic focusing ensure that most molecules will pass the detection volume, making this method applicable for detection of trace amounts of molecules.

Secondly, surface-immobilized molecules can be detected using screening stages. For this purpose, distinct areas of a glass surface are functionalized with capture agents, e.g. antibodies, specific ligands, or cDNA. This procedure allows for parallel investigation of a large number of different fluorescence labeled target molecules on one chip. The basis for ultra-sensitive chip read-out are techniques for detecting single molecules on surfaces. In initial studies, confocal microscopy was used to efficiently discriminate single molecule signals from background. The method is based on scanning a diffraction limited laser focus over the sample; the fluorescence emitted from the sample is imaged via a

pinhole onto a point detector [23,24]. Using Avalanche Photodiodes (APD) as detectors allows to obtain additional information about the excited state lifetime. Combination of several APDs placed after a stack of dichroic and polarization beam splitters was used to maximize the information content acquired from a single molecule [17]. However, due to the serial data acquisition the inspection of large sample areas remains a time-consuming task. The time T required for recording an area A at a resolution δ and an illumination time t_{ill} can be calculated according to $T = A/\delta^2\, t_{ill}$. For $\delta = 320$ nm and $t_{ill} = 10$ ms, the time for recording an area $A = 1$ cm^2 in a confocal set-up is equal to 9.9×10^6 s (corresponding to 3.8 months).

In a different approach, several groups utilized intensified or back-illuminated CCD-cameras for imaging single molecules on surfaces [8–10,25–27]. Large sample areas are illuminated with a defocused laser spot and directly imaged. This simultaneous observation was the methodological prerequisite for tracking individual molecules moving in planar systems. In screening assays, parallel observation of many pixels dramatically reduces the recording time T, compared to confocal methods. T can be estimated using the formula $T = A/\delta^2 N \cdot [t_{ill} + Nt_{read\text{-}out} + Lt_{line\text{-}shift} + t_{positioning}]$, with N the overall number of pixels on the camera chip. The sum represents contributions of the illumination time (t_{ill}), the time to digitize each pixel ($t_{read\text{-}out}$), the time to shift one line into the read-out register ($t_{line\text{-}shift}$) and additional terms accounting for positioning the stage, subsumed in $t_{positioning}$; L gives the total number of lines on the chip.

The principal advantage of using pixel arrays as detectors is parallel signal acquisition. Still, the pixel array covers only a small part of the sample area A to be imaged, making additional scanning of the sample inevitable. A proper way for reducing overhead times due to stage positioning and signal integration is the implementation of synchronized continuous stage-shift and camera read-out (H. Schindler, international patent PCT/AT9900257). It is based on the so-called time-delayed-integration (TDI) mode, and allows to decrease the recording time to $T = A/\delta^2 N \cdot [Nt_{read\text{-}out} + Lt_{line\text{-}shift}] \approx 1000$ s, corresponding to 16.7 min (assuming a commercial available NTE/CCD 1340×100, Roper Scientific, with $t_{read\text{-}out} = 1$ μs and $t_{line\text{-}shift} = 12$ μs). In the direction of scanning, the intensity profile of the excitation beam needs not to be constant. In practice, it is convenient to use a Gaussian profile with a width of $\omega \approx L\delta/2$. This ensures maximum excitation of dye molecules within the region of observation, and at the same time minimum photobleaching of dyes in regions still to be scanned. In TDI mode, the illumination time is not well-defined. Basically, it is given by the time required to move each molecule through the excitation beam. In order to allow comparison between TDI mode and conventional imaging, we define here an effective illumination time for TDI mode, $\hat{t}_{ill}$: given an image recorded in TDI mode, $\hat{t}_{ill}$ represents the illumination time in conventional imaging for recording an image of the same quality. Or, in mathematical terms: if $n_h = I_{max}t_{ill}$ represents the number of excitation cycles in a homogenous excitation beam profile of intensity I_{max}, and $n_i = \int I(x)\, dt$ the number of excitation cycles in TDI mode, the effective illumination time is given by the time for which n_h equals n_i, i.e. $n_h(\hat{t}_{ill}) = n_i$. Assuming a Gaussian beam profile with $I(x) = I_{max} \exp\left[-x^2/\omega^2\right]$, the effective illumination time is given by $\hat{t}_{ill} = I_{max}/\int I(x)/v\ dx = \sqrt{\pi}\omega/v = \sqrt{\pi}\omega/\delta L \cdot [Nt_{read\text{-}out} + Lt_{line\text{-}shift}]$. For the NTE/CCD 1340×100, $\hat{t}_{ill}$ equals 60 ms.

If the fluorescence intensity, F, would scale linearly with illumination intensity, I, i.e. $F \propto It_{ill}$, confocal scanning microscopy could be performed at the same speed as camera-based systems. In this linear regime, focusing of the laser spot by a factor N yields an increased excitation intensity NI, which allows to reduce t_{ill} by a factor N for constant fluorescence emission. However, for high speed single molecule detection it is favorable to operate at illumination intensities close to the saturation intensity of the fluorophore I_S, i.e. $F \propto (1 + I_S/I)^{-1} t_{ill}$ [28]. In this case, increase of the intensity has minor effects on F, therefore the illumination time may not be reduced in order to ensure constant signal. Evidently, non-linear effects make camera-based detection systems preferential for ultra-sensitive high-throughput screening. It is interesting to note, that for conventional dyes used in ultra-sensitive spectroscopy, the time required to photobleach the fluorophore at illumination intensities close to I_S is shorter than $\hat{t}_{ill}$ [29]. Therefore, all photons emitted from a molecule until

photobleaching contribute to the signal, yielding maximum signal levels.

The image of a single dye molecule is represented by a diffraction limited spot on the camera. Automatic fitting algorithms have been developed which allow to determine the position of individual molecules to an accuracy of ~50 nm. For unambiguous single molecule probing, the concentration has to be much less than $1/\delta^2$ to ensure that the signals of two molecules do not overlap. Assuming equal distribution of molecules on a surface, the probability that the distance to the nearest neighbor is larger than the size of the diffraction limited spot of $r = 500$ nm is given by $F_{nn}(r) = \exp\left(-r^2 \pi n\right)$ [30], with n the concentration of dye molecules. For a certainty $F > 95\%$, n has to be less than 1 molecule/15 μm^2.

In order to achieve single molecule sensitivity, the transmission efficiencies of all optical elements in the detection path have to be maximized. In general, the overall detection efficiency, η, can be separated into three factors: the efficiency of the microscope objective, η_O, of optical filters, η_F, and of the detector, η_D. Typical values are: $\eta_O \sim 30\%$ for an oil immersion objective with NA = 1.4, $\eta_F \sim 50\%$, $\eta_D \sim 80\%$, yielding $\eta \sim 12\%$. Obviously, the limiting factor is the objective, which collects only a minor fraction of all emitted photons due to the limited collection angle set by the numerical aperture. At optimized settings, such systems allow to obtain images of single dye molecules in synthetic environments at a high signal to background ratio of ~50. Besides high detection efficiencies, this is mainly related to the low noise characteristics of cooled CCD cameras.

Fig. 1 shows a schematic view of the apparatus developed in our lab, here termed ''Nanoreader'': laser light is coupled into an epi-fluorescence microscope, and the emitted light is detected after appropriate filtering on the pixel array of a CCD camera. The excitation beam is defocused to match the region of observation defined by the size of the CCD-array and the chosen magnification of the objective. A homogenous beam profile perpendicular to the scanning direction is achieved using an aspherical lens as beam shaper. For optimum resolution, the step-size of the high precision scanning stage has to fit the pixel size in the image plane, δ. In addition, an

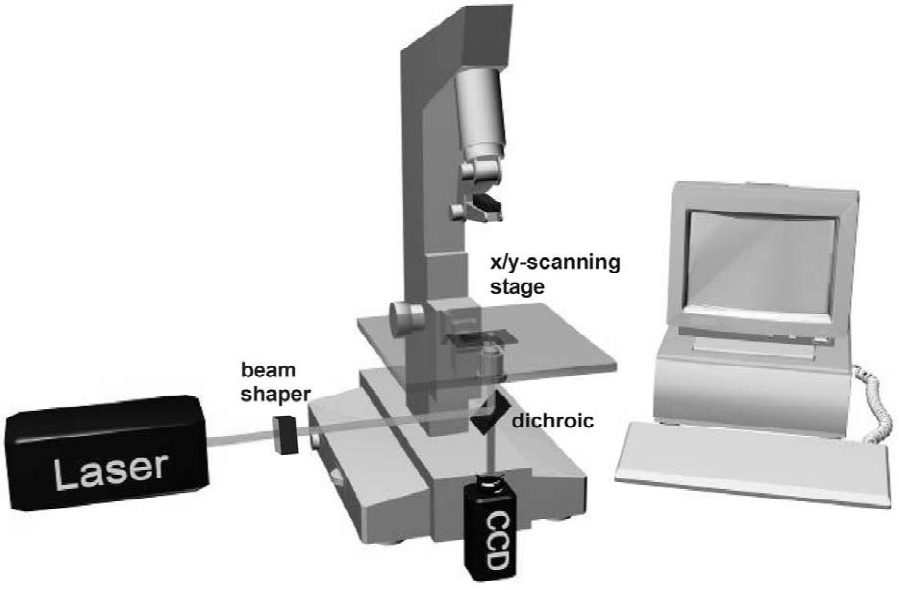

Fig. 1. Scheme showing the general set-up of the ''Nanoreader''. The laser beam is shaped with aspherical lenses to the desired line-profile, and projected onto the sample. Fluorescence emission is collected through a high NA objective and, after appropriate filtering, imaged onto a back-illuminated high QE CCD camera. For TDI mode, a high precision scanning stage is synchronized with the read-out of the camera.

autofocus system was introduced to correct for thickness-variations or tilts of the supporting chip-surface. It is based on rapidly refocusing the microscope objective during the scan process. Distance changes of the glass surface from the objective are measured using a second laser at a different wavelength focused onto the chip surface. Angular changes of the back-reflected beam are detected on a two-segment photodiode and corrected by shifting the objective [31].

Lipid bilayers represent a highly defined model system for single molecule microscopy [32]. They allow to precisely adjust the surface density down to very low concentrations of about one fluorescent molecule per 100 μm^2. Fig. 2 shows a supported lipid bilayer made of dipalmitoylphosphocholine (DPPC), containing a molar ratio of $\sim 10^{-8}$ of the fluorescent analog dipalmitoylphosphoethanolamine-(DPPE-) Cy5. An area of 200×600 μm was recorded in one scan using TDI-mode (A). The main part of the scan area is covered by the bilayer. There, individual DPPE-Cy5 molecules can easily be discriminated as sharp peaks with a signal-to-noise ratio of ~50 in the zoom-in (B). A few aggregates, however, can be observed as signals of much higher brightness in (A).

The scanning process introduces minor distortions broadening the peaks in the scanning direction by ~200 nm (C). Two major contributions for peak broadening have to be considered. Firstly, the scanning stage moves continuously, while lines are shifted stepwise on the CCD chip, which introduces blur of up to 1 pixel in the scanning direction. Secondly, non-perfect mechanics and optics might account for slight dephasing of the scanning stage and the CCD-camera. This effect can be minimized

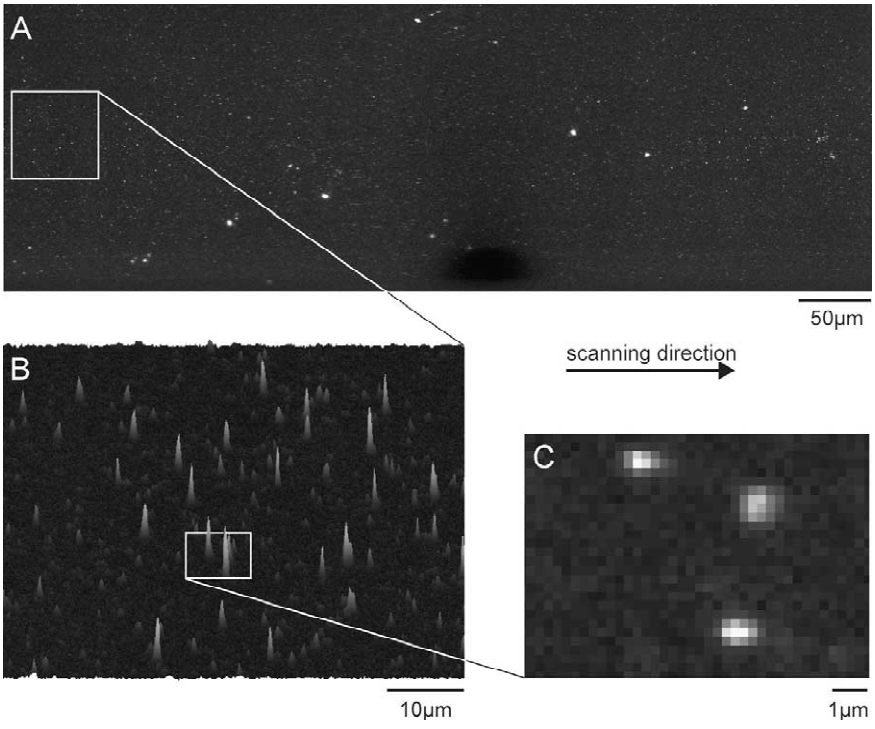

Fig. 2. A 200×600 μm scan (A) of single Cy5-labeled lipid molecules (DPPE-Cy5) embedded in a supported lipid membrane of DPPC, obtained with the ''Nanoreader''. The molar ratio of $\sim 10^{-8}$ allows to easily discriminate individual molecules as diffraction limited peaks at a signal to background ratio of ~50, as apparent from the 60×60 μm detail shown in (B). Due to the scanning process, the peak shape is slightly broadened in the scanning direction by ~200 nm (C; see text for details).

by adjusting the magnification of the optical system to fit the demands set by the scanning stage.

3. Information contained in single molecule images

The fluorescence image of a dye molecule contains two parameters accessible by a camera as a detector: firstly, the *position* of the molecule, which is given by the center of its signal. This can be determined to an accuracy much below the wavelength of light; ~40 nm can be achieved routinely for positioning single biomolecules at room temperature using wide field microscopy [33]. Secondly, its *fluorescence intensity*, which can be quantified by the number of photons detected from the molecule during the illumination time. This number can be taken as a characteristic property of the dye molecule under constant environmental conditions. A third parameter, the *fluorescence lifetime*, is up to now only measurable using point detectors; for a critical discussion of the implications of lifetime analysis for single molecule studies we refer to Refs. [6,17]. In the following, several aspects of single molecule studies based on these observables will be highlighted.

3.1. Local stoichiometry

In general, a single dye molecule emits a well-defined number of photons during a given illumination time, which can be taken as a characteristic parameter of the molecule. The fluorescence signal obtained from a single molecular structure can thus be used as a measure for the number of bound fluorophores. This principle has been employed in rather different fields like rapid sizing of fluorescently stained DNA-fragments [34], as well as molecular counting of low-density lipoprotein particles on cell surfaces [35]. The critical point in all methodologies utilizing fluorescence intensity for sizing is the reliability of assignment. Using randomly labeled particles, the accuracy of discrimination between n and $n+1$ associated particles scales with $N^{0.5}$, with N representing the mean number of fluorophores per particle. Therefore, high discrimination accuracy requires heavily labeled particles.

In the single fluorophore regime, reliable stoichiometric assignment is possible by using labeling at a defined ratio. The reliability then depends only on the inherent intensity fluctuations of the dye molecule used. In this regime of very low fluorescence intensities, the stochastic nature of photon emission leads to statistical distributions of the actual detected fluorescence, which can be characterized and taken into account for assignment of local stoichiometries. Using the approach of single molecule counting, the number of fluorescence labeled ligands bound to individual membrane anchored receptor molecules could be determined, allowing for digital analyte quantitation on a molecular level [36].

3.2. Co-localization of different molecules

Two different strategies have been employed to study colocalization of different molecules: single pair fluorescence resonance energy transfer (FRET) [37] and dual wavelength imaging [38]. FRET between donor and acceptor dyes, also termed Förster energy transfer [39], is, in application to ensembles, a well-established assay for the study of colocalization or clustering of components in, for example, cell membranes [40–42]. Recently, FRET was carried to the ultimate limit of the energy transfer between a single pair (donor–acceptor) of biomolecules (single pair FRET; for a review see Ref. [43]). The strong distance dependence between donor and acceptor molecule on length scales of ~5 nm was utilized to quantify distances on single DNA molecules [37,44], to observe conformational dynamics on single enzymes [45], and to image ligand colocalization on individual receptor molecules [46]. Even first applications to living cells have been demonstrated recently [11].

Dual wavelength imaging, the alternative approach to colocalization, visualizes the positions of two different dye molecules in the same probe. The two images are acquired either consecutively [46] or simultaneously [38,47–49] by imaging the same sample area containing two different dyes using two spectroscopic channels specific for the two fluorophores.

3.3. Orientation

Light absorption of a fluorophore depends on the angle between the polarization of the excitation light and the orientation of the transition dipole of the dye. Using linear polarized light for excitation allows to determine the orientation of a single fluorescent dye by measuring the modulation of the fluorescence signal [50–53]. This is equivalent with measuring the linear dichroism of a single dye. In addition, the polarization of the fluorescence signal emitted from the fluorophore can be determined by introducing a polarizing beam-splitter in the emission path of the microscope [54–56]. This methodology has been applied for determination of the axial rotation of actin filaments sliding along myosin molecules [56], for monitoring conformational changes in single myosin molecules [54], for observing subunit rotation of enzymes [57], and for observation of the rotational diffusion of individual lipids in an artificial lipid membrane [55]. Combination of both polarized excitation and determination of the emission polarization allows for steady state anisotropy measurements on a single molecule [55,58], which opens the possibility to access nanosecond time-scales for probing single molecule reorientation. In addition, determination of the polarization can be performed for two colors simultaneously [17,47]. This allows combined measurements of dye orientation and energy transfer, yielding much deeper insights into molecular reorganizations of large biomolecules.

The basic limitation of this approach is its restriction to the study of the in-plane component of the orientation of a dye molecule. In conventional wide field microscopy, the polarization of the excitation light lies mainly in the focal plane. Attempts to access the full orientation of a molecule are therefore based on methodologies with a high *z*-component in the polarization, like near field microscopy [59,60] or modified confocal microscopy [61]. From the image pattern, the azimuth and elongation angle of a dye molecule can be calculated.

4. Application to genomics/proteomics

Chip-technology has become the prevalent method for investigation of differential gene expression [62] and proteomics [63]. Its current applicability, however, is restricted by the large amounts of sample required. The development of new platforms for high-throughput identification and characterization of biomolecules at lowest concentrations is one major research goal in biotechnology. Such a device represents the technical environment for a ''lab on the chip''. Rapid identification and quantification of all bound protein molecules define the required specification of this readout device. Currently, planar waveguide-based excitation allows quantification of protein amounts on chip surfaces down to 500 molecules per spot of 150 μm diameter [4]. Ultimately, individual molecules will be bound to distinct loci on the chip.

The tremendous sensitivity of single molecule microscopy enables the investigation of samples containing only trace amounts of proteins. For estimation, we will describe briefly the binding of proteins in solution to a chip surface coated with a high density of specific antibodies. Using first order binding kinetics, one obtains for the surface density of bound proteins, $\rho_{Ab\text{-}P}$

$$\rho_{Ab\text{-}P} = \frac{Ab + P + VK_{\mathrm{D}}N_{\mathrm{A}}}{2A} - \sqrt{\left(\frac{Ab + P + VK_{\mathrm{D}}N_{\mathrm{A}}}{2A}\right)^2 - \frac{PAb}{A^2}} \quad (1)$$

with Ab, the number of immobilized antibodies, P the number of protein molecules in solution, A the area of the antibody spot on the chip, V the volume of the protein solution, K_{D} the dissociation constant, and N_{A} the Avogadro-number. Application of a sample containing only 300 molecules of a specific protein onto a protein chip will result in ~75 protein molecules bound to a distinct capture area of $\sim 10^4$ μm^2.

To ensure optimum binding conditions, local densities of ~1 antibody per 100 nm^2 are assumed, yielding a final amount of $\sim 10^6$ capture antibodies per spot. Fig. 3 shows the theoretical calibration curve for an overall sample volume of 1 nl, a capture antibody density of 1/100 nm^2, a K_{D} of 1 n*M*, and a spot size of 10 μm (solid line) and 100 μm (dashed line). The spot size can be used to adjust the linear region for optimum quantification. The overall binding efficiency covers a range of six orders of

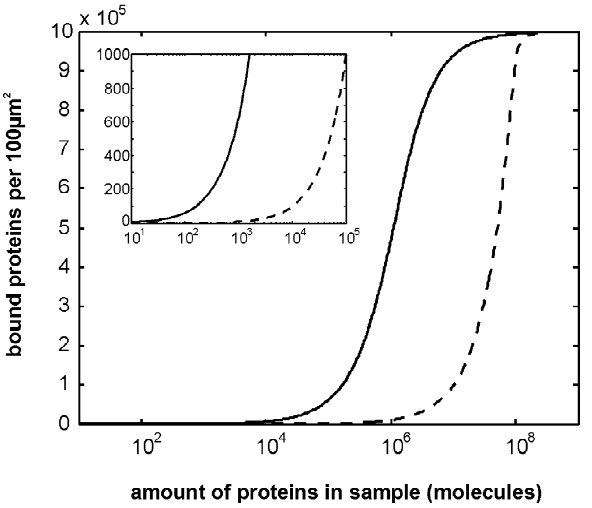

Fig. 3. Figure of merit for protein profiling. The binding curve shows the number of protein molecules immobilized on the capture area, as a function of the amount contained in the sample. The solid (dashed) line was calculated for a spot size of 10 μm (100 μm), using Eq. (1). For both curves, an overall sample volume of 1 nl, a capture antibody density of 1/100 nm^2 and a K_D of 1 n*M* were assumed. At low concentrations, the sensitivity of the ''Nanoreader'' is inevitable for quantification (insert).

magnitude, which fits to the dynamic range of the ''Nanoreader''.

Single molecule microscopy requires new strategies for image analysis. Firstly, low signal levels have to be identified and quantified over a background of random noise by implementing new fitting algorithms. Secondly, the sheer amount of data produced in high resolution imaging demands for digital pre-processing to enable rapid data analysis.

The increased information content of single molecule measurements compared to experiments on ensembles of molecules allows to design novel types of assays. Additional screening parameters come into reach, like receptor occupancies, colocalization of different ligands on one receptor, or even details like receptor–ligand-orientations. The full impact of this new information for drug-screening—but also medical diagnostics—has yet to be proven. Single molecule screening techniques have shown their feasibility for routine measurements in a scientific environment; for their general application, however, easy-to-use systems still have to be developed. In combination with novel software algorithms, ultrasensitive imaging techniques are foreseen to become standard equipment for laboratories performing biological diagnostics.

Acknowledgements

We would like to thank Mark Christenson (Roper Scientific) for continuous technical help and Amersham Pharmacia Biotech for general support. This work was funded by the Austrian Research Funds, grant P15053, and the State of Upper Austria.

References

[1] R.L. Strausberg, J. Pathol. 195 (2001) 31.
[2] B. Schweitzer, S. Roberts, B. Grimwade, W. Shao, M. Wang, Q. Fu, Q. Shu, I. Laroche, Z. Zhou, V.T. Tchernev, J. Christiansen, M. Velleca, S.F. Kingsmore, Nat. Biotechnol. 20 (2002) 359.
[3] Z. Zhang, S. Krylov, E.A. Arriaga, R. Polakowski, N.J. Dovichi, Anal. Chem. 72 (2000) 318.
[4] M. Pawlak, E. Schick, M.A. Bopp, M.J. Schneider, P. Oroszlan, M. Ehrat, Proteomics 2 (2002) 383.
[5] W.E. Moerner, L. Kador, Phys. Rev. Lett. 62 (1989) 2535.
[6] W.E. Moerner, M. Orrit, Science 283 (1999) 1670.
[7] E.B. Shera, N.K. Seitzinger, L.M. Davis, R.A. Keller, S.A. Soper, Chem. Phys. Lett. 174 (1990) 553.
[8] I. Sase, H. Miyata, J.E. Corrie, J.S. Craik, K. Kinosita Jr., Biophys. J. 69 (1995) 323.
[9] T. Funatsu, Y. Harada, M. Tokunaga, K. Saito, T. Yanagida, Nature 374 (1995) 555.
[10] T. Schmidt, G.J. Schutz, W. Baumgartner, H.J. Gruber, H. Schindler, Proc. Natl. Acad. Sci. USA 93 (1996) 2926.
[11] Y. Sako, S. Minoghchi, T. Yanagida, Nat. Cell. Biol. 2 (2000) 168.
[12] G.J. Schutz, G. Kada, V.P. Pastushenko, H. Schindler, EMBO J. 19 (2000) 892.
[13] G.J. Schutz, V.P. Pastushenko, H.J. Gruber, H.-G. Knaus, B. Pragl, H. Schindler, Single Mol. 1 (2000) 25.
[14] S. Nie, D.T. Chiu, R.N. Zare, Science 266 (1994) 1018.
[15] E. Bismuto, E. Gratton, D.C. Lamb, Biophys. J. 81 (2001) 3510.
[16] S. Wennmalm, L. Edman, R. Rigler, Proc. Natl. Acad. Sci. USA 94 (1997) 10641.
[17] C. Eggeling, S. Berger, L. Brand, J.R. Fries, J. Schaffer, A. Volkmer, C.A. Seidel, J. Biotechnol. 86 (2001) 163.
[18] U. Haupts, S. Maiti, P. Schwille, W.W. Webb, Proc. Natl. Acad. Sci. USA 95 (1998) 13573.
[19] J. Korlach, P. Schwille, W.W. Webb, G.W. Feigenson, Proc. Natl. Acad. Sci. USA 96 (1999) 8461.
[20] O. Krichevski, G. Bonnet, Rep. Prog. Phys. 65 (2002) 251.
[21] M. Auer, Drug Discov. Today 6 (2001) 935.

[22] A. Van Orden, R.A. Keller, W.P. Ambrose, Anal. Chem. 72 (2000) 37.
[23] M. Minsky, Scanning 10 (1988) 128.
[24] J.B. Pawley, Handbook of Biological Confocal Microscopy, Plenum, New York, 1995.
[25] X.H. Xu, E.S. Yeung, Science 275 (1997) 1106.
[26] R.M. Dickson, A.B. Cubitt, R.Y. Tsien, W.E. Moerner, Nature 388 (1997) 355.
[27] R.M. Dickson, D.J. Norris, Y.L. Tzeng, W.E. Moerner, Science 274 (1996) 966.
[28] T. Schmidt, G.J. Schutz, W. Baumgartner, H.J. Gruber, H. Schindler, J. Phys. Chem. 99 (1995) 17662.
[29] C. Eggeling, J. Widengren, R. Rigler, C.A. Seidel, Anal. Chem. 70 (1998) 2651.
[30] S. Chandrasekar, Rev. Mod. Phys. 15 (1943) 1.
[31] E.H. Hellen, D. Axelrod, Rev. Sci. Instrum. 61 (1990) 3722.
[32] G.J. Schutz, M. Sonnleitner, P. Hinterdorfer, H. Schindler, Mol. Membr. Biol. 17 (2000) 17.
[33] G.J. Schutz, H. Schindler, T. Schmidt, Biophys. J. 73 (1997) 1073.
[34] P.M. Goodwin, M.E. Johnson, J.C. Martin, W.P. Ambrose, B.L. Marrone, J.H. Jett, R.A. Keller, Nucl. Acids Res. 21 (1993) 803.
[35] D. Gross, W.W. Webb, Biophys. J. 49 (1986) 901.
[36] T. Schmidt, G.J. Schutz, H.J. Gruber, H. Schindler, Anal. Chem. 68 (1996) 4397.
[37] T. Ha, T. Enderle, D.F. Ogletree, D.S. Chemla, P.R. Selvin, S. Weiss, Proc. Natl. Acad. Sci. USA 93 (1996) 6264.
[38] T. Ha, T. Enderle, D.S. Chemla, S. Weiss, IEEE J. Select. Top. Q.E. 2 (1996) 1.
[39] T. Förster, Ann. Physik 6 (1948) 55.
[40] A.K. Kenworthy, M. Edidin, J. Cell. Biol. 142 (1998) 69.
[41] D.L. Taylor, Y.-L. Wang, Fluorescence Microscopy of Living Cells in Culture Part B, Academic Press, San Diego, 1989.
[42] N.P. Mahajan, K. Linder, G. Berry, G.W. Gordon, R. Heim, B. Herman, Nat. Biotechnol. 16 (1998) 547.
[43] T. Ha, Methods 25 (2001) 78.
[44] A.A. Deniz, M. Dahan, J.R. Grunwell, T. Ha, A.E. Faulhaber, D.S. Chemla, S. Weiss, P.G. Schultz, Proc. Natl. Acad. Sci. USA 96 (1999) 3670.
[45] T. Ha, A.Y. Ting, J. Liang, W.B. Caldwell, A.A. Deniz, D.S. Chemla, P.G. Schultz, S. Weiss, Proc. Natl. Acad. Sci. USA 96 (1999) 893.
[46] G.J. Schutz, W. Trabesinger, T. Schmidt, Biophys. J. 74 (1998) 2223.
[47] L. Cognet, G.S. Harms, G.A. Blab, P.H. Lommerse, T. Schmidt, Appl. Phys. Lett. 77 (2000) 1.
[48] T. Enderle, T. Ha, D.S. Chemla, S. Weiss, Ultramicroscopy 71 (1998) 303.
[49] K. Saito, M. Tokunaga, A.H. Iwane, T. Yanagida, J. Microsc. 188 (1997) 255.
[50] G.J. Schutz, H. Schindler, T. Schmidt, Opt. Lett. 22 (1997) 651.
[51] A.G.T. Ruiter, J.A. Veerman, M.F. Garcia-Parajo, N.F. van Hulst, J. Phys. Chem. 101 (1997) 7318.
[52] T. Ha, T. Enderle, S. Chemla, R. Selvin, S. Weiss, Phys. Rev. Lett. 77 (1996) 3979.
[53] F. Güttler, J. Sepiol, T. Plakhotnik, H. Mitterdorfer, A. Renn, U.P. Wild, J. Lumin. 56 (1993) 29.
[54] D.M. Warshaw, E. Hayes, D. Gaffney, A.M. Lauzon, J. Wu, G. Kennedy, K. Trybus, S. Lowey, C. Berger, Proc. Natl. Acad. Sci. USA 95 (1998) 8034.
[55] G.S. Harms, M. Sonnleitner, G.J. Schutz, H.J. Gruber, T. Schmidt, Biophys. J. 77 (1999) 2864.
[56] I. Sase, H. Miyata, S. Ishiwata, K. Kinosita Jr., Proc. Natl. Acad. Sci. USA 94 (1997) 5646.
[57] K. Adachi, R. Yasuda, H. Noji, H. Itoh, Y. Harada, M. Yoshida, K. Kinosita Jr., Proc. Natl. Acad. Sci. USA 97 (2000) 7243.
[58] T. Ha, J. Glass, T. Enderle, S. Weiss, Phys. Rev. Lett. 80 (1998) 2093.
[59] J.A. Veerman, M.F. Garcia-Parajo, L. Kuipers, N.F. van Hulst, J. Microsc. 194 (1999) 477.
[60] E. Betzig, R.J. Chichester, Science 262 (1993) 1422.
[61] B. Sick, B. Hecht, L. Novotny, Phys. Rev. Lett. 85 (2000) 4482.
[62] D.J. Lockhart, E.A. Winzeler, Nature 405 (2000) 827.
[63] G. MacBeath, S.L. Schreiber, Science 289 (2000) 1760.